

ULTRAFAST TRANSMISSION ELECTRON MICROSCOPY

A.A. Ischenko^{1,@}, L. Schäfer², Yu.I. Tarasov¹, E.A. Ryabov³, S.A. Aseyev³

¹Moscow Technological University (Institute of Fine Chemical Technologies), Moscow, 119571 Russia

²Department of Chemistry and Biochemistry, University of Arkansas, Fayetteville, AR, U.S.A., AR72701

³Institute of Spectroscopy of the RAS, Moscow, Troitsk, 108840 Russia

@Corresponding author e-mail: aischenko@yasenevo.ru

Ultrafast laser spectral and electron diffraction methods complement each other and open up new possibilities in chemistry and physics to light up atomic and molecular motions involved in the primary processes governing structural transitions. Since the 1980s, scientific laboratories in the world have begun to develop a new field of research aimed at this goal. "Atomic-molecular movies" will allow visualizing coherent dynamics of nuclei in molecules and fast processes in chemical reactions in real time. Modern femtosecond and picosecond laser sources have made it possible to significantly change the traditional approaches using continuous electron beams, to create ultrabright pulsed photoelectron sources, to catch ultrafast processes in the matter initiated by ultrashort laser pulses and to achieve high spatio-temporal resolution in research. There are several research laboratories all over the world experimenting or planning to experiment with ultrafast electron diffraction and possessing electron microscopes adapted to operate with ultrashort electron beams. It should be emphasized that creating a new-generation electron microscope is of crucial importance, because successful realization of this project demonstrates the potential of leading national research centers and their ability to work at the forefront of modern science.

Keywords: ultrafast electron diffraction, crystallography and microscopy, ultrashort laser pulses, femtosecond and picosecond pulsed electron beams, ultrafast photoexcitation of molecules, coherent dynamics of nuclei, coherent electron dynamics, dynamics of phase transitions.

СВЕРХБЫСТРАЯ ПРОСВЕЧИВАЮЩАЯ ЭЛЕКТРОННАЯ МИКРОСКОПИЯ

А.А. Ищенко^{1,@}, заведующий кафедрой, Л. Шефер², профессор, Ю.И. Тарасов¹, заведующий кафедрой, Е.А. Рябов³, заведующий отделом лазерной спектроскопии, С.А. Асеев³, ведущий научный сотрудник лаборатории спектроскопии ультрабыстрых процессов

¹Московский технологический университет (Институт тонких химических технологий), Москва, 119571 Россия

²Факультет химии и биохимии, Университет штата Арканзас, Фэйтвилл, 72701, Арканзас, США

³Институт спектроскопии РАН, Москва, Троицк, 108840 Россия

@Автор для переписки, e-mail: aischenko@yasenevo.ru

Методы сверхбыстрой электронной дифракции, лазерной спектроскопии и квантовой химии, дополняя друг друга, открывают новые возможности изучения внутримолекулярной динамики веществ, участвующих в процессах химических реакций. Переходное состояние химических реакций определяет направление этих процессов. Начиная от первых работ 1980-х годов, выполненных в России и показавших принципиальную возможность исследования когерентной динамики ядер молекулярных систем, многие научные лаборатории в мире начали интенсивную разработку новой области исследований, направленную на экспериментальное исследование переходного состояния методом сверхбыстрой дифракции электронов. Последовательное развитие этого направления привело к созданию так называемого "атомно-молекулярного кино", позволяющего визуализировать когерентную динамику ядер в молекулах и сверхбыстрые процессы в химических реакциях в режиме

реального времени. В настоящее время ряд научно-исследовательских лабораторий в мире разрабатывают методы сверхбыстрой дифракции электронов и рентгеновского излучения, которые открыли возможность исследования переходного состояния химических реакций. Создание электронных микроскопов с высоким пространственно-временным разрешением является новым направлением в электронной микроскопии, близко примыкающим к этому новому направлению науки. Успешная реализация этого направления исследований демонстрирует потенциал ведущих национальных научно-исследовательских центров и их способность работать на переднем крае современной науки.

Ключевые слова: сверхбыстрая дифракция электронов и рентгеновского излучения, кристаллография и электронная микроскопия, ультракороткие лазерные импульсы, фемтосекундные и пикосекундные импульсные электронные пучки, сверхбыстрое фотовозбуждение молекул, когерентная динамика ядер, когерентная динамика электронов, динамика фазовых переходов.

CONTENTS

Introduction
1. Transmission and scanning electron microscopy
2. 4D Electron microscopy
3. Examples of instrument designs
4. Applications of time-resolved microscopy
4.1. Phase transitions in nanoparticles
4.2. Laser-induced crystallization
4.3. Musical nanoscale instruments: a drum, a harp and a piano
4.4. 4D Electron tomography
4.5. Plasmonics, nanophotonics and topological phase of matter
4.6. Imaging of isolated molecules with ultrashort pulsed photoelectron beam
5. Future trend
5.1. Spatial and temporal electron microscopy with additional spectral resolution
5.2. Controlling the motions of free electrons by femtosecond light pulses
Conclusions
Acknowledgements
References

Introduction

The goal of any microscopy is to study the structure, composition, and a variety of physical and chemical properties of materials, biological samples, or other microscopic items [1–3]. Conventional microscopy can capture static images of structures on length scales in the micrometer regime for optical microscopes and nanometer, or even sub-nanometer scales, with electron microscopes. Traditional microscopy aims to observe snapshots of the microscopic world, frozen in time. It is the goal of ultrafast electron microscopy to add a temporal dimension to those observations, i.e. to observe the motions of nanoscale objects.

In most conventional microscopies, electromagnetic radiation or corpuscular beams act as the probes: optical microscopes use light while electron microscopes use

electron beams for imaging, respectively. Other microscopic methods take advantage of ions, protons, positrons, neutrons, or acoustic or microwave radiation or other, less common, methods [3–8]. In each of them, the specificity of the interaction of a beam of particles (or photons) and the molecules or atoms of a sample yield unique and rather useful information about the structure, composition and microscopic inhomogeneities of the sample, and the nature of their intermolecular interactions [5, 6, 9]. Scanning probe microscopies, which use a sharp probe tip that is scanned across surfaces, are fundamentally quite different and possibly more difficult to adapt to the time domain.

Imaging in classical microscopy is achieved in either of two ways: In transmission mode, a large area of the sample is illuminated by a beam of light or particles and the image of the object is projected onto a screen or detector by specifically designed lenses. In reflection mode, either the primary radiation reflected off the sample, or secondary particles or photons generated by the incident beam, are used to form an image of the sample [1, 10]. Most often, transmission microscopes that use, for example, a film, photographic plate, photosensitive recorder or digital camera, produce the entire image at once [11, 12]. Reflection microscopes often operate in “scanning microscopy” mode, where the sample is scanned by a beam focused to a spot of rather small diameter, and the resulting image is assembled point by point.

Because most materials absorb the optical radiation, transmission optical microscopy is limited to sample thicknesses of typically less than 1 mm. In electron microscopy, the sample has to be much thinner because the electrons interact with matter more strongly than light. Transmission electron microscopy is therefore applicable only to very thin slices, with film thicknesses of much less than 1 micrometer. Such samples are prepared using special ultramicrotomes that can produce film thicknesses down to a few tens of nanometers [2].

1. Transmission and scanning electron microscopy

Scanning microscopes form images by focusing a beam of charged particles or photons to a very small

diameter and moving it across the surface of an object. Reflected particles or photons are recorded by a detector that does not require imaging capability. The image is constructed "point by point" by recording the signal as a function of the probe beam position. The method is reminiscent of the generation of an image using a scanning electron beam in a traditional cathode ray tube (CRT), or the modulation of the brightness of luminous points in a LCD monitor [13]. Scanning microscopy is a rather convenient tool to study the morphology and topography of various geometric objects, to investigate elemental compositions, to measure the electric and magnetic fields in micro-volumes, or to test electrical parameters such as lifetime diffusion length of charge carriers in semiconductor crystals [14].

In a transmission electron microscope (TEM), an electron beam illuminates a larger area of a very thin sample. As they are relayed by a set of electrostatic or magnetic lenses onto a fluorescent screen or equivalent position sensitive detector, the transmitted electrons form an image [2, 15]. The first such transmission electron device was demonstrated in 1931 by M. Knoll and E. Ruska [16], who imaged a wire mesh using an electron beam. The image was formed by an axially symmetric set of magnetic electron lenses with a narrow annular gap and a sharp maximum of the magnetic field on the axis. The first commercial transmission electron microscope was developed and released by Siemens A.G. in 1939 under the supervision of E. Ruska, who received the Nobel Prize for Physics in 1986 for his design of the electron microscope.

The transmission electron microscope is the now a ubiquitous tool that finds applications in the study very thin samples and nanoscale structures with typical dimensions of about 10-100 nm. Using electron accelerating voltages of up to 200 kV [17], the electron rays of the microscope are quite similar to those of optical light microscopes in that they create an image of the sample based on the transmitted beam, Fig. 1 [17].

The transmission electron microscope consists of an electron gun and an assembly of electromagnetic lenses. Fig. 1 shows the path of the rays in a microscope with three levels of zoom and one condenser lens that is used to pre-focus of the electron beam. The two common modes of operation are the imaging mode and the micro-diffraction mode. In imaging mode, the plane of the sample conjugates to the screen where the image is formed. It is assumed that the sample is very thin compared to the focal length of the imaging objective lens. In diffraction mode, the sample conjugates to the back focal plane of the objective lens, where the distribution of the amplitudes of the electron beam corresponds to the Fraunhofer diffraction of the electrons by the sample [1].

The diffraction mode makes possible the chemical analysis of very small samples [18]. The phrase "micro-diffraction" is often invoked, where the word "micro" implies

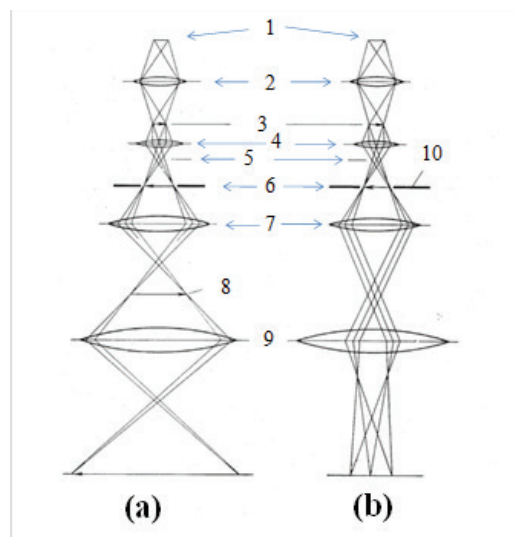


Fig. 1. The ray paths in the transmission electron microscope and its modes of operation:

- (a) – imaging the spatial structure of the sample;
 (b) – micro-diffraction: 1 – the source of the electrons;
 2 – the condenser lens; 3 – the sample;
 4 – the object lens; 5 – the focal plane of the object lens;
 6 – the first intermediate image; 7 – the intermediate lens;
 8 – the second intermediate image;
 9 – the projection lens; 10 – the selector diaphragm.

that the diffraction signal is observed from only a rather small area of the sample. The area is chosen either by a special selector diaphragm that is placed in the plane of the first intermediate image (see Fig. 1), or by irradiation of the desired part of the sample with a tightly focused electron beam.

In imaging mode, a so-called aperture diaphragm is installed in the focal plane of the object lens in order to limit the aperture of the beam, i.e. the opening angle of the cone of rays emerging from the sample. This helps to decrease the spherical aberration, a basic imaging error that is associated with the projection of a point in the sample to a point of the image [1, 19]. Fig. 1 presents the setup with the single-lens condenser. Modern microscopes are usually equipped with a two-lens condenser that allows for a rather high electron flux to a small area of the object with characteristic size of 1-5 microns. This eliminates problems arising from the growth of films due to hydrocarbon polymerization of oil vapors as a result of electron bombardment of the unobserved sample areas in instruments where the microscope column is evacuated by diffusion pumps.

The most common electron microscopes, of which many thousands have been produced, use electron accelerating voltages of 80-100 keV. Several hundred instruments with an accelerating voltage of between 200 keV and 500 keV were created for the study of objects with thicknesses of up to 10 microns. Comparatively few microscopes with voltages in the MeV range have been built.

The electrons of a typical transmission microscope with an accelerating voltage of 100 keV have a de Broglie wavelength of 3.7 pm. This is much smaller than the order of 100 pm diameter of a hydrogen atom. Experience with optical microscopes, where the resolution is limited by the wavelength of the light, might suggest it is easy to observe any atomic particle with an electron microscope. But instead, it is extremely difficult to observe individual atoms. This is because the spatial resolution is limited by the poor quality of electron lenses compared to optical lenses: at the same angular size of the light and electron beams, electron lenses create almost of two orders of magnitude more aberrations and image distortion [1, 15, 19].

2. 4D Electron microscopy

To observe the motions of microscopic systems in a dynamical fashion, one encounters a challenge with a well known tradition. While the human eye can follow slow processes, events that happen on time scales faster than about a tenth of a second elude our direct observation. To probe temporal events faster than that, the English photographer Eadweard Muybridge invented the use of multiple cameras. As an example, Fig. 2 shows an 1871 Muybridge recording that captures the moment when a galloping horse separated all four hooves from the surface of the earth.

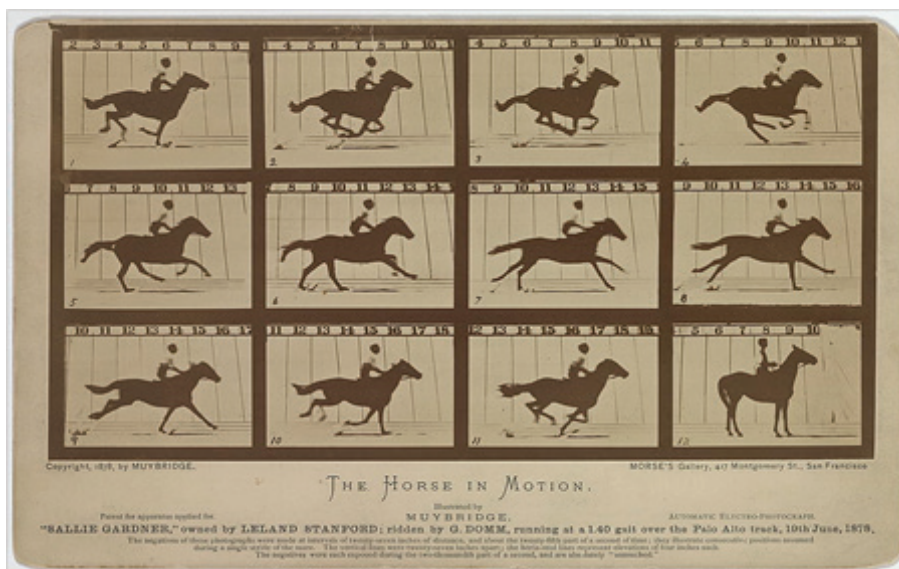


Fig. 2. One of the first “movies” in history. These images were obtained by E. Muybridge in 1871. The time delay between the exposures was about 50 ms [20].

Of scientific interest today would be movies showing the movement of atoms in molecules, the fast dynamical processes in biological systems, or the changes in the geometrical structures of nanoscale devices. To estimate the magnitudes of time scales involved, we can extrapolate from the observation of macroscopic objects by using as the maximum velocity the speed of sound. Thus, if a time resolution of 1 μ s suffices to time-freeze the motions of objects with spatial dimensions of 1 mm, then in a system with a characteristic length scale of nanometers, a picosecond (10^{-12} s) time resolution is appropriate. To resolve the motions of individual atoms and functional groups within molecular systems, a time resolution in the femtosecond regime is necessary.

The two principal designs of electron microscopes, the scanning design and the transmission microscope [1, 2], can each be adapted to a time resolved operation. However, for all but the slowest processes of interest, scanning an electron beam even as the molecular dynamical process is unfolding, would be too slow. Consequently, the scanning approach is best implemented with temporal processes that are repetitive:

in a stroboscopic microscope, the scan of the electron beam and the associated detection of back-reflected primary and secondary radiation are synchronized with the oscillatory motions of the nanoscale object of interest. In contrast, a transmission microscope, which can capture an entire image at once, does not require repetitive processes. That approach is used in the so-called dynamical transmission electron microscope [21]. Both types of instrument will be discussed in detail below.

To illustrate the main components of an ultrafast electron microscope, Fig. 3 shows the schematic of a recently built instrument that was designed to explore phenomena occurring on a picosecond or sub-picosecond time scale [4, 22].

The instrument can conceptually be divided into three components: (1) the electron gun, where the sub-picosecond pulsed electron beam is formed and accelerated to a high energy; (2) the interaction unit, in which the sample is excited by femtosecond laser pulses and its spatial-temporal structure probed by ultrashort electron bunches; and, in this case, (3) the position-

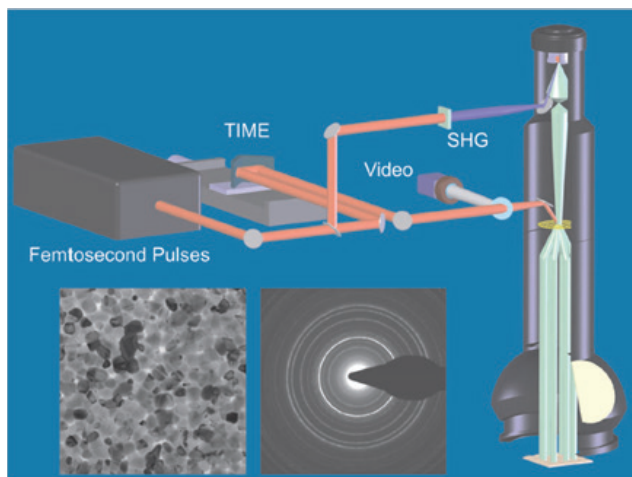


Fig. 3. Schematic illustration of an ultrafast electron microscope. A commercial electron microscope, operating in a continuous mode, can be taken as a basis in order to create such a device. To adapt it to time-resolved microscopy requires a femtosecond laser to provide a pulsed excitation of the sample (laser beam shown in red), and another one for the preparation of the photoelectron probe pulse of ultrashort duration (marked in blue) [23]. (Reprinted figure with permission from [Grinolds M.S., Lobastov V.A., Weissenrieder J. and Zewail A.H. Four-Dimensional Ultrafast Electron Microscopy of Phase Transitions // Proc. Nat. Acad. Sci. U.S.A. 2006. V. 103. P. 18427-18431]. Copyright (2006) National Academy of Sciences, U.S.A).

sensitive detection of the electrons after their interaction with the sample. In other designs, the backscattered or secondary electrons will be observed.

The use of electron beams consisting of short electron pulses imposes strict requirements on the detector, because such pulses cannot sustain a large number of electrons. To make up for this constraint, the detection efficiency of the detector should be as high as possible. After much development work, the detection efficiency for the time-resolved instrument, illustrated in Fig. 3, has been improved by almost an order of magnitude compared to that of a standard electron microscope [4]. In addition to enabling the time resolved experiments, the low electron flux also provides interesting opportunities in areas where radiation damage is of concern, such as in the imaging of biological samples.

The generation and propagation of ultrashort electron bunches are at the core of time-resolved electron microscopy. We will therefore pay special attention to the effects that need consideration in the design of an instrument [24]. The duration of the photoemission of electrons from the surface of a solid cathode, and therefore the initial duration of the photoelectron bunch, is determined by the duration of the laser pulse. But during the propagation from the photocathode to the target, the electron beam is stretched in time. We shall

consider three major factors that lead to a smearing of the electron bunch.

First, the acceleration of photoelectrons in a static electric field near the solid photocathode causes so-called time-of-flight chromatic aberrations (TFCA). The temporal spreading of the electron pulse is given by:

$$\Delta\tau_{\text{EF}} = \sqrt{2m_e\Delta E_e}/eF, \quad (1)$$

where ΔE_e is the initial spread of the kinetic energy of the electrons as they emerge from the cathode and F is the electric field in the acceleration gap.

This expression for TFCA can be obtained by solving a quadratic equation that describes the uniformly accelerated motion of the electrons in the acceleration gap of the length of l :

$$v_0t + (eF/m_e)t^2/2 = l$$

Differentiating the both sides with respect to time t yields:

$$\Delta v_0 + (eF/m_e)\Delta t \approx 0,$$

from which the expression for TFCA immediately follows. As a numerical example let us consider an electron pulse with an initial energy spread of $\Delta E_e = 0.3$ eV, which is accelerated by a field of $F \approx 10^8$ V/m. This is about the maximum value of the field as higher values lead to vacuum breakdown even with special electrodes that have undergone thorough mechanical, electrochemical and ionic treatment. With those parameters, eq. (1) suggests a broadening of the pulse by $\Delta\tau_{\text{EF}} \approx 60$ fs.

Secondly, the travel of electrons with slightly different kinetic energies through the field-free flight tube requires a fair amount of time, during which the electrons drift apart. The resulting elongation of the electron pulse during this time of flight is expressed as:

$$\Delta\tau_{\text{TOF}} = t_{\text{TOF}}(\Delta E_e/2K). \quad (2)$$

Here, t_{TOF} is the travel time of the electrons with kinetic energy K from the photocathode to the sample. Any temporal spreading after the sample is of no consequence. As an example, using electrons with kinetic energy $K = 30$ keV, an energy spread of $\Delta E_e = 0.3$ eV as above, and a travel time $t_{\text{TOF}} \approx 3$ ns that corresponds to a distance of 30 cm between the cathode and the target, one obtains $\Delta\tau_{\text{TOF}} \approx 15$ fs.

Thirdly, the Coulomb repulsion between the electrons that comprise a pulse causes a swelling of the pulse. To estimate the effect of this space-charge interaction on the temporal properties of the beam, we

consider a model in which the electron bunch is traveling through a field-free region. The total energy of the bunch, consisting of N electrons, is conserved:

$$V + W = \frac{1}{2} \sum e^2 / 4\pi\epsilon_0 |\mathbf{r}_i - \mathbf{r}_j| + \frac{1}{2} \sum m_e v_i^2 \quad (3)$$

Therefore, the characteristic value of the distribution of the velocities, δv , resulting from the electrons pushing each other apart, is qualitatively estimated as:

$$m_e \delta v^2 / 2 \approx e^2 N / (16\pi\epsilon_0 \delta r), \quad (4)$$

where δr is the initial size of the photoelectron cloud. In this model, the velocity spread of the electrons causes an elongation of the order of $\Delta\tau_C \approx t_{TOF} \delta v / v_e$, which can be rewritten as:

$$\Delta\tau_C = (t_{TOF} / v_e) \sqrt{e^2 N / (8\pi\epsilon_0 \delta r m_e)} \quad (5)$$

As an example, consider an instrument with $N \approx 10^4$ electrons moving with a velocity of $v_e \approx 10^8$ m/s for a flight time of $t_{TOF} \approx 3$ ns. Let us assume that initially, the electron pulse is confined to an initial size of $\delta r \approx 10$ μm , which might result from the tight focusing of a laser beam on a photocathode. Within the framework of the simple model, we find that the space-charge interactions lead to a broadening of the electron pulse by $\Delta\tau_C \approx 5$ ps.

These considerations, and the numerical examples, suggest that the Coulomb repulsion of the electrons within each electron bunch is the main factor that constrains the design of ultrafast electron microscopes. Of course, various parameters can be optimized, although in most cases there are trade-offs to be considered. For example, the use of very high accelerating voltages, such as 500 keV instead of 30 keV, can reduce the swelling of the electron bunch due to Coulomb repulsion; but it can also lead to enhanced damage of the sample. Use of very fast electrons, in the MeV range, can further reduce the space-charge broadening because of the onset of relativistic effects [25, 26]. It should also be noted that an electrostatic mirror, a so-called reflectron, can be used to re-compress the electron bunches after their original spreading [27, 28]. At the present time, a radio frequency compression scheme is already in use for this purpose.

Visualizing the rearrangement of atoms in different molecular and condensed-matter systems requires resolving picometre displacements on a 10-fs timescale [29]. The authors of this work demonstrated the compression of single-electron pulses with a de Broglie wavelength of 0.08 \AA to a full-width at half-maximum duration of 28 fs, substantially shorter than most phonon periods and molecular normal modes. These measurements pave the way to resolve the fastest

atomic motions relevant in reversible condensed-matter transformations and organic chemistry.

An important challenge in the field of 4D, i.e. spatially and temporally resolved, electron microscopy remains the observation of an image or a diffraction pattern produced by a single electron pulse. While for pulses of long (nanosecond) duration this has been achieved using conventional electron acceleration voltages [30], meeting this challenge for ultrashort, i.e. picosecond or femtosecond pulses, is more difficult. A solution to this problem is rather important, because it would enable the study of ultrafast irreversible processes. An early breakthrough has been achieved by a collaboration of scientists at Brown University and at SLAC, who used ultrashort electron pulses with 5.4 MeV of energy, generated using the Gun Test Facility at SLAC, to record single-shot diffraction patterns of 160 nm thick aluminum foils [25, 26]. Their work showed that MeV electrons should make it possible to achieve sub-100 fs time resolution using single shot images. Subsequently, physicists in Japan, applying a magnetic sector to compress the electron bunches, were able to collect diffraction patterns of thin gold films with single, subpicosecond electron bunches [31].

3. Examples of instrument designs

Conventional electron microscopes take advantage of two of the three main properties of the electron: the small de-Broglie wavelength, which enables very high spatial resolution; and the electric charge, which allows one to control its movement by electric and magnetic fields [1]. Already 60 years ago, a third important property of the electron, its small mass and the concomitant low inertia, began to be used in so-called *stroboscopic electron microscopy* for the study of periodic processes [32]. The essence of the method is quite simple: a sample with periodically time-varying characteristics, with a fixed rate of change, is irradiated by short bunches of electrons that arrive at the sample with the same frequency and with a fixed phase relationship. The synchronicity of the periodic processes and the electron probe bunches effectively freezes the image, which shows the state of the sample at the time of arrival of the electron pulses.

Stroboscopic techniques were developed in the Soviet Union as early as the 1960's by G.V. Spivak. All major types of electron microscopes were adapted to this purpose [33, 34]. These developments allowed the exploration of many processes in rapidly varying thin films and in surface layers of solids. Examples include the re-polarization of ferroelectrics, the distinctions of the domain structure during re-magnetization of thin magnetic films, the heterogeneity of alternating fields of magnetic heads, and the local defects of p-n junctions during their fast switching between the locked and open states [35].

The initial work on stroboscopic microscopy was in the microsecond and nanosecond time regime.

Subsequently, several laboratories started to push into the picosecond domain, usually using stroboscopic scanning electron microscopy to investigate periodic processes. The main difficulties arose from the gating, the interruption, or the modulation of the electron beam. Two methods can be used for this: first, one can change the intensity of the electron beam by applying appropriate voltage pulses across the cathode or across a modulator in the electron gun; and secondly, one can deflect a continuous electron beam by an electric or magnetic field in the vicinity of a skipping aperture of small diameter. The electron pulses so obtained should, of course, be properly frequency and phase synchronized with the periodicity of the sample to avoid a loss of resolution.

The larger the duty cycle of the blanking pulses, i.e. the higher the ratio of the repetition period to the duration of the front of the electron pulse, the better the temporal resolution of the stroboscopic microscope, but the lower the brightness of the image. Consequently, each application requires a careful assessment of the best trade-offs. Moreover, a very short front of the pulse causes the resolution of the microscope to deteriorate because of non-ideal edges of the pulse, the appearance of chromatic aberration in transmission electron microscopy and the manifestation of the Boersch-effect [36], i.e. the transition of the longitudinal component of the electron velocity to a transverse component due to Coulomb repulsion.

Space-charge effects can be completely eliminated by using electron pulses that contain, in the extreme limit, only a single electron. If the pulse train has a large enough number of electron pulses then the overall current must not necessarily be small. Zewail and his group have demonstrated this approach [37,38] by using a femtosecond laser pulse train with 80 million pulses per second to generate a current in the range of 500 pA, implying about 40 electrons per pulse. This microscope delivers not only excellent temporal resolution but also a very high spatial resolution.

While the stroboscopic approach is limited to repetitive signals to which the electron pulse train is locked in frequency and phase, a different approach, called *dynamic transmission electron microscopy* (DTEM), enables the capture of images that follow one-time events [21]. Just as Muybridge's temporally sequenced image frames were the predecessors of real movies, so it can be expected that the step-by-step acquisition of images can eventually lead to the creation of the long-desired 'molecular movies'.

A review article [21] and monograph [4] describe the development of the methods of 4D, dynamic transmission electron microscopy. A sketch of a DTEM is reproduced in Fig. 4. In the DTEM approach, the cathode drive laser pulse is sufficiently intense to generate an electron bunch that contains a large number

of electrons. This pulse is accelerated toward the sample, and just as in standard transmission electron microscopy, the transmitted electrons are projected onto a screen using a set of electrostatic lenses.

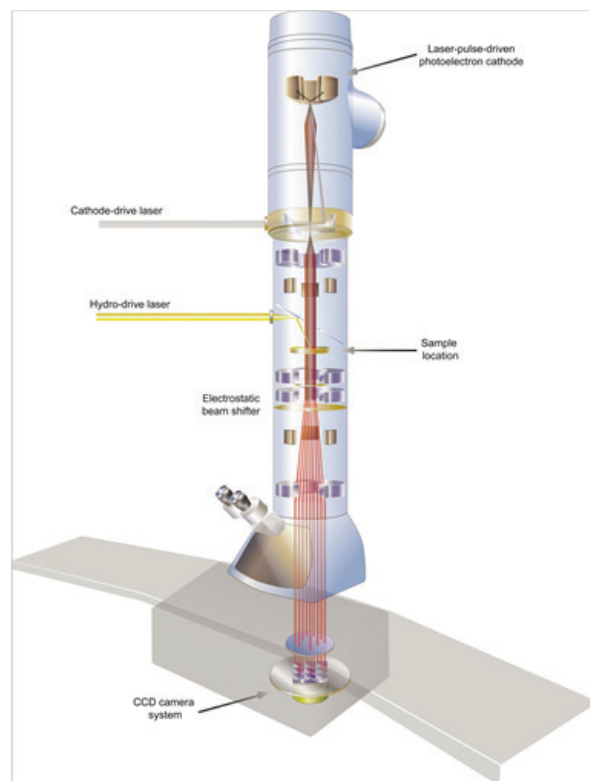


Fig. 4. The schematic of a dynamic transmission electron microscope (DTEM) [21].

A challenging aspect of the DTEM design is to minimize space-charge interactions between the electrons vis-à-vis the need to have a sufficient number of electrons to obtain an image. In the instrument shown in Fig. 4, this is achieved by operating the device with electron pulse durations of 10's of nanoseconds. Such long pulses can sustain the requisite electron numbers, on the order of 108 electrons, to make imaging possible with a single shot.

Quite recently a compact electron source specifically designed for time-resolved diffraction studies of free-standing thin films and monolayers has been developed [39]. An extremely compact design, in combination with low bunch charges, allows for high quality diffraction in a lensless geometry.

A further important technological advance embodied in the instrument of Fig. 4 relates to the recording of the transmitted electrons. The problem with a conventional detector capturing the transmitted electron image is that the readout of the detector must be sufficiently fast to follow the fast repetition rate of the electron bunches. To solve this problem, the design of Fig. 4 uses a deflector system to cast images from different electron bunches onto different parts of the detector, so that an un-gated

CCD camera can be used to capture multiple shots. As illustrated below, the nanosecond time resolution of the instrument is sufficient to explore many phenomena in material science, such as the propagation of melting fronts upon localized heating. The DTEM approach with the multi-frame detector is attractive also because it approaches the ultimate goal of recording movies of one-time events.

In 2016, at the Institute for Spectroscopy of Russian Academy of Sciences (ISAN) it has been created ultrafast transmission 75-keV photoelectron microscope in collaboration with the Moscow Technological University (MIREA), Institute of Fine Chemical Technologies. The setup is based on commercial transmission electron microscope Hitachi H-300 and is intended for the researches of dynamic processes in the solids by excitation of a sample

by femtosecond laser pulses and with probing emerging dynamics using ~ 7 ps pulsed photoelectron beam. The introduction of an adjustable optical delay between excitation and probing channels enables observation of ultrafast processes in matter. Our apparatus has been combined with 80-MHz femtosecond laser Mai-Tai, 2.5-MHz femtosecond fiber laser Antaus, or 1-kHz source of amplified femtosecond laser pulses with an energy of up to 4 mJ per laser pulse. In the first part of the experiments it has been visualized the interaction of picosecond 75-keV electron beam with charged cloud emitted from copper target under the action of focused femtosecond laser radiation. In the next part, the laser-induced plasma and associated processes in the vicinity of solid target will be investigated with high spatio-temporal resolution.

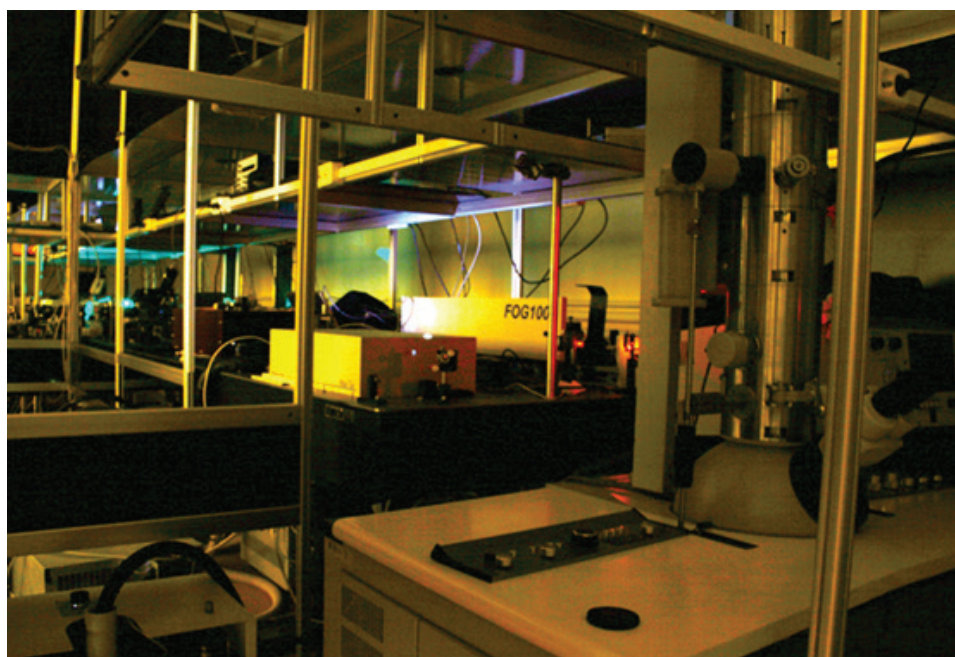


Fig. 5. Overview of the ultrafast transmission electron microscope at Institute of Spectroscopy of the Russian Academy of Sciences developed by research group from ISAN and Moscow Technological University, Institute of Fine Chemical Technologies.

4. Applications of time-resolved microscopy

4.1. Phase transitions in nanoparticles

When vanadium dioxide, VO_2 , is heated beyond 67°C , it undergoes a phase transition of the first type, reorganizing from a low-temperature monoclinic structure (M) to a high-temperature tetragonal rutile structure (R). The studies [23] describe the application of ultrafast electron microscopy to explore this phase transition. Since those studies used single electron probe pulses, Coulomb space-charge problems were absent. The authors were able to record a time series of images, i.e. a movie, with a very high spatial resolution and an ultrashort temporal resolution. They also showed that it was possible to investigate an ultrafast metal-insulator phase transitions in the same material. A structural

phase transition in VO_2 nanoparticles is manifest in the diffraction patterns (at atomic scale) and in the microscope images (on a nanometer scale) with a temporal resolution on the order of 100 fs (Fig. 6).

This time-resolved ultrafast electron microscopy study recorded the motion of atoms upon femtosecond laser irradiation of the sample in the near IR, revealing the phase transition in all three dimensions and in time. It showed that as an initial step, the vanadium atoms are separated from each other, and subsequently begin to move towards their final positions.

Phase-change materials represent the main candidates for data storage devices with high-speed recording performance, which use the large difference in the physical properties of their transitional lattice structures. On a nanoscale, it is fundamental to determine

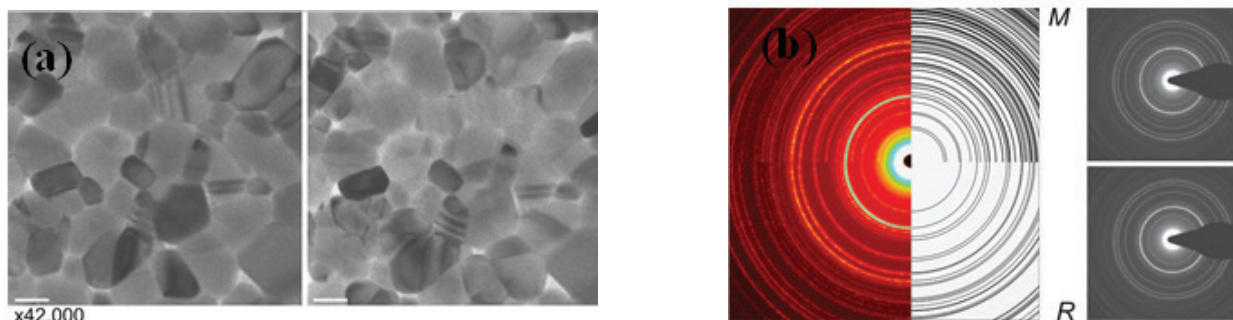


Fig. 6. (a) Images showing a phase transition in the films of VO_2 (left) and after the phase transition (right), were collected with a magnification of 42 000 (the bar corresponds to 100 nm). (b) The diffraction patterns, corresponding to the phase transition in the films of VO_2 (right) and after the phase transition (left).

The monoclinic phase and the high-temperature rutile phase are experimentally observed (left side of panel (b)) and constructed by calculations, right side of panel (b). From [23]. (Reprinted figure with permission from [Grinolds M.S., Lobastov V.A., Weissenrieder J. and Zewail A.H. Four-Dimensional Ultrafast Electron Microscopy of Phase Transitions // Proc. Nat. Acad. Sci. U.S.A. 2006. V. 103. P. 18427-18431].

Copyright (2006) National Academy of Sciences, U.S.A.)

their performance, which is ultimately controlled by the speed limit of transformation among the different structures involved. In the work [40], the authors report observation with atomic-scale resolution of transient structures of nanofilms of crystalline germanium telluride, using ultrafast electron crystallography. A nonthermal transformation from the initial rhombohedral phase to the cubic structure was found to occur in about 12 ps. On a much longer time scale (hundreds of picoseconds) equilibrium heating of the sample is reached, driving the system toward amorphization. Thus it is possible to visualize the elementary steps defining the structural pathway in the transformation of crystalline-to-amorphous phase transitions.

4.2. Laser-induced crystallization

Capturing movies of nanoscale objects undergoing irreversible dynamical processes is one of the essential goals of time resolved electron microscopy. The dynamic TEM equipped with a multi-frame detector described above (Fig. 4) enables the recording of brief image sequences that can be assembled to a movie. The work [30] describes the observation of irreversible phase transitions resulting from the rapid heating of a sample with a short laser pulse. Specifically, the authors reported the observation of crystallization in GeTe, Fig. 7. The sequence of images spans the time range from slightly before the exposure of the sample by the laser to about 2.5 μs after the irradiation event. During this time, the laser pulse heats the sample to more than 800 K, at the center of the laser beam profile. The material responds by undergoing a phase transition to form crystallized GeTe, a process that unfolds on a microsecond time scale. Since this time scale is much longer than the duration of each electron bunch, 17.5 ns, each exposure freezes the motions in time, resulting in spatially well-resolved images.

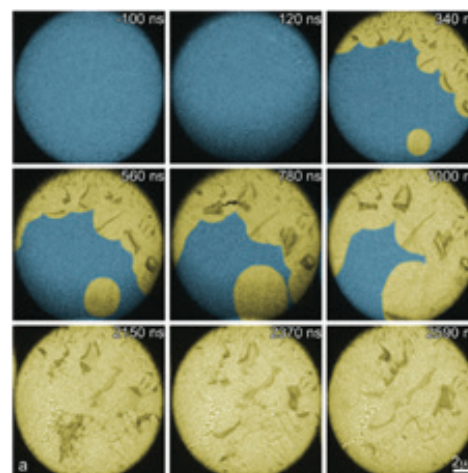


Fig. 7. Frames of a ‘movie’ revealing the crystallization of amorphous GeTe (blue) into crystalline regions (yellow) after exposure of the material to laser pulses with 4.7 mJ of energy. The individual frames were recorded in the work [30] using 17.5 ns electron pulses deflected onto different detector areas at the time points as indicated.

The recent progress in ultrafast and ultrabright electron and x-ray sources makes it possible to extend crystallography to the femtosecond time domain in order to literally light up atomic motions involved in the primary processes governing structural transitions [41]. The advances in this area have enabled atomic resolution to structural dynamics for increasingly complex systems. Corresponding scientific activity focuses on achieving sufficient brightness in pump-probe schemes to resolve the far-from-equilibrium motions directing chemical processes that in general lead to irreversible changes in different samples. Given the central importance of structural transitions to conceptualizing chemistry, this emerging field in science has the potential to significantly improve our understanding of chemistry.

4.3. Musical nanoscale instruments: a drum, a harp and a piano

Most materials subjected to an ultrashort, intense laser pulse experience strains that result from the non-uniform spatial and temporal distributions of the absorbed laser energy and from changes in the lattice parameters induced by the sudden deposition of energy. For very small structures, the accompanying deformations may be very large. Using ultrathin platelets of graphite and gold, Baskin with the co-workers [42] have used the effect in a surprising way. In their experiments, graphite nano-sheets with thicknesses of 75 nm were exposed to pulsed laser radiation with a wavelength of 532 nm and a repetition rate of 5 kHz [4]. The energy density of the focused laser pulses reached a value of about 7 mJ/cm², an exposure that led to mechanical vibrations. Using 200-keV electrons, Baskin with the colleagues [42] were able to image these vibrations, see Fig. 8.

Baskin et al. observed that immediately following the exposure to the laser pulse, individual carbon atoms vibrated in a random order. But after a few tens of

microseconds, the corresponding modes of the graphite membrane began to synchronize (Fig. 8). Apparently, the graphite sheet resembles a "drumbeat" – albeit with a much higher frequency than found in a macroscopic drum: the frequency of the nanoscale graphite membrane is around 1 MHz.

To process the images of Fig. 8, a cross-correlation function was defined as:

$$\gamma(t';t) = [\sum_{x,y} C_{x,y}(t)C_{x,y}(t')]/\sqrt{[\sum_{x,y} C_{x,y}(t)^2 \sum_{x,y} C_{x,y}(t')^2]}, \quad (6)$$

where the contrast is:

$$C_{x,y}(t) = [N_{x,y}(t) - \langle N(t) \rangle] / \langle N(t) \rangle.$$

Here, $N_{x,y}(t)$ is the number of counts corresponding to the picture element (pixel) with the coordinates of (x, y), and $\langle N(t) \rangle$ is the average number of the counts. To assemble Fig. 8, 2000 images had to be collected with time interval of 50 ns. The micrograph of the graphite membrane itself is represented in the lower left corner of Fig. 8.

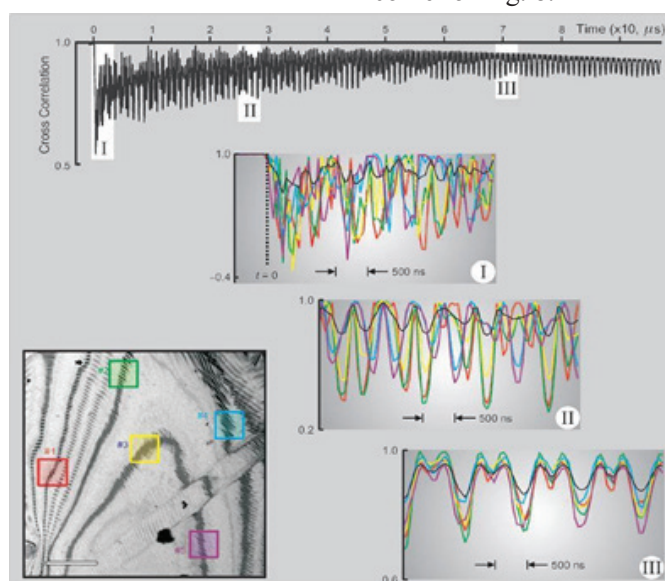


Fig. 8. The time-dependence of the oscillatory motions of graphite membranes, as represented by the cross-correlation functions. The scale bar in the lower left figure indicates a length of 5 microns. Five areas that feature different initial dynamics are marked in red, yellow, green, blue and purple. The transition from chaotic behavior to coherent oscillations is shown in the panels I-II-III. They correspond to different temporal intervals as indicated in the top panel. From [42]. (Reprinted with permission from (Baskin J.S., Park H.S., and Zewail A.H. Nanomusical Systems Visualized and Controlled in 4D Electron Microscopy // Nano Lett. 2011. V. 11. No. 2. P. 2183-2191).

Copyright (2011) American Chemical Society).

Following the success with the graphite sheet nano-drum, other nanoscale musical instruments were constructed using arrays of cantilevers (Fig. 9.) The devices were created from micro-structuring of multilayer work-pieces of Ni/Ti/Si₃N₄ using sharply-focused ion beams [42]. Each work-piece consisted of 30 nm layers of nickel and titanium that had been applied to 15 nm films of Si₃N₄. To create a 'piano', the cantilevers

had almost the same lengths, approximately 4.6 μm, but their width varied from about 400 nm to 2.3 μm. To generate a 'harp', the lengths and widths of individual elements varied in the range of 1.2 - 9.1 μm and ~ 300-600 nm, respectively.

To 'play' the instruments, the harp and the piano were exposed to nanosecond 519 nm (or 532 nm) pulses from a Nd:YAG laser that arrived at 1 ms

intervals and that carried energy densities per pulse of 2 mJ/cm^2 . Aided by the layered structures with different coefficients of thermal expansion, the laser exposures induced mechanical deformation that launched the vibrations. The motions of the oscillators were observed

using the synchronized electron microscope. The results for individual cantilevers p1, p5, h1 and h5 as indicated in Fig. 9 are shown in Fig. 10. An analysis of the dependence of the oscillatory frequencies on the device dimension is provided in Fig. 11.

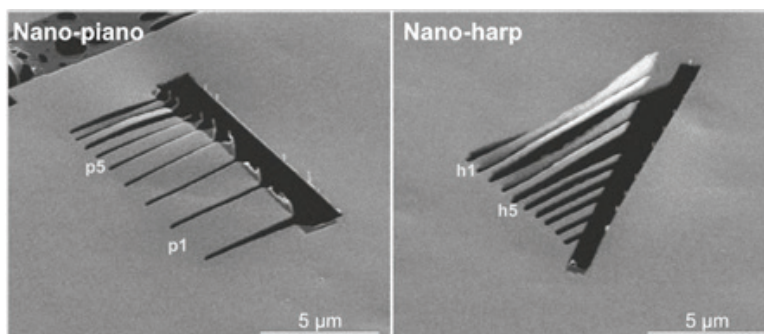


Fig. 9. Images of nanoscale musical instruments, obtained with a scanning electron microscope.

Note that two of the thinnest cantilevers, p7 and p8 on the left, and two pairs of cantilevers, h1/h2 and h3/h4 on the right, are partially melted in the central part as a result of micro-structuring by the focused ion beam [42]. (Reprinted with permission from (Baskin J.S., Park H.S., and Zewail A.H. *Nanomusical Systems Visualized and Controlled in 4D Electron Microscopy* // *Nano Lett.* 2011. V. 11. No. 2. P. 2183-2191). Copyright (2011) American Chemical Society.)

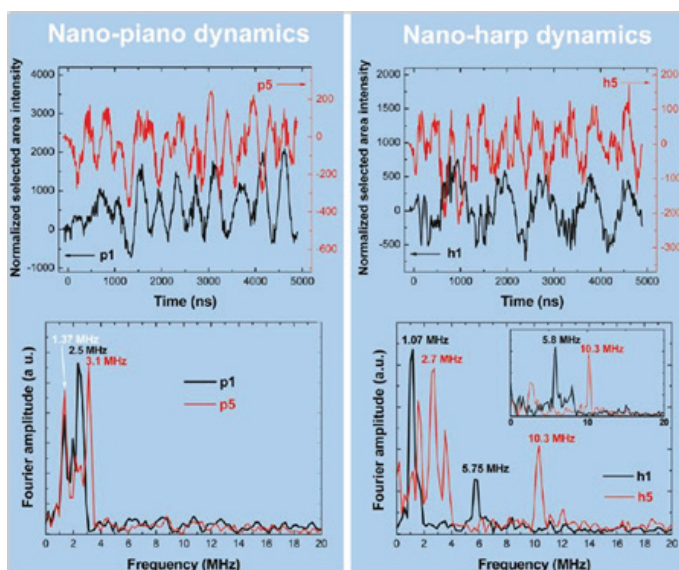


Fig. 10. Oscillations of cantilevers caused by the pulsed heating of the sample (top) and the fast Fourier transform of the motions, bottom. The experimental data are provided for a selection of the structures as labeled in Fig. 9 [42]. (Reprinted with permission from (Baskin J.S., Park H.S., and Zewail A.H. *Nanomusical Systems Visualized and Controlled in 4D Electron Microscopy* // *Nano Lett.* 2011. V. 11. No. 2. P. 2183-2191). Copyright (2011) American Chemical Society.)

Beyond the pure pleasure of marvelling at the richness of phenomena in the microscopic world, nanoscale oscillatory systems can also have very important applications. For example, Baskin et al. [42] note that the layered nanostructures could be used to precisely measure the temperature of a device with a spatial dimensions of $10 \mu\text{m}$, even while maintaining a microsecond temporal resolution.

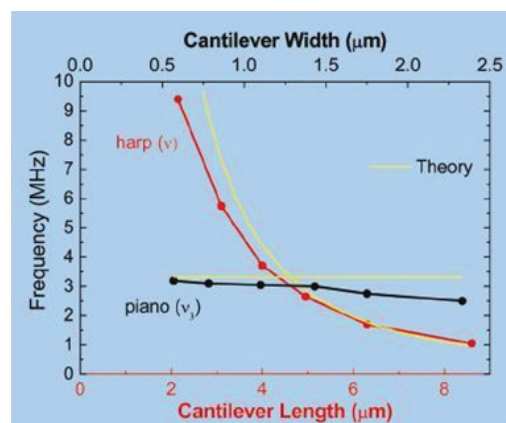


Fig. 11. The dependence of the oscillatory frequency on the size of the cantilever. Only out-of-plane vibrations are represented [42]. (Reprinted with permission from (Baskin J.S., Park H.S., and Zewail A.H. *Nanomusical Systems Visualized and Controlled in 4D Electron Microscopy* // *Nano Lett.* 2011. V. 11. No. 2. P. 2183-2191). Copyright (2011) American Chemical Society.)

4.4. 4D Electron tomography

Tomographic measurements, i.e. the mapping of three dimensional structures using electrons, date back to as early as the 1960-ies [43]. Since the analysis of the data involves the processing of a large number of 2-dimensional electron diffraction patterns, progress had been limited mainly by the lack of computer power. But the development of modern computational capabilities

has changed the situation, to the point where it is now possible to add the fourth dimension, time, using the methodology of time-resolved microscopy.

To record a 3D image of a nanoscale object, the object needs to be probed by the electron beam from different directions, see Fig. 12.

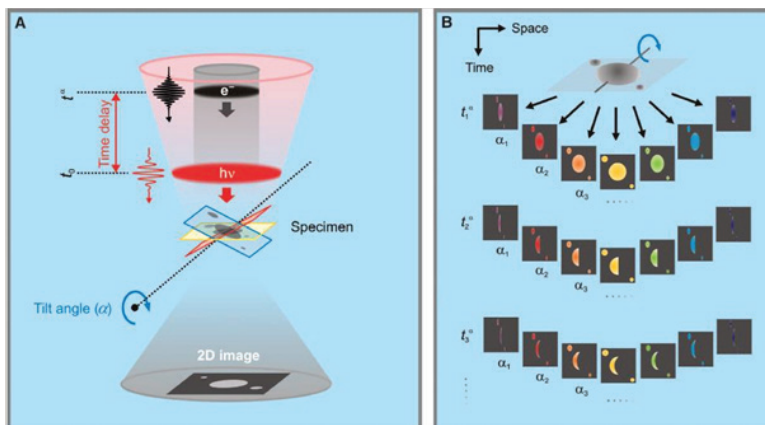


Fig. 12. (A) Schematically, 4D electron tomography employs short laser pulses to induce a dynamical change, followed by a short electron pulse a short time afterward. To record the tomographic image, the object needs to be observed from different vantage points, which can be achieved by rotating it about a tilt angle, α . (B) Here the series of two-dimensional electronic images can be taken at different angles α and time delays. In the work of [44], the angle is varied from -58° to $+58^\circ$ in 1° increments, requiring a total of 4000 projections.

Applying the concepts of 4D electron tomography, [44] studied the temporal behavior of carbon nanotubes. A nanotube of length $L \approx 4.4 \mu\text{m}$ was twisted in the form of a bracelet. Here the images in Fig. 13 and 14 were obtained using electron pulses with an energy of 200 keV.

Exposure of the sample to a femtosecond laser pulse heated the nanotube and caused structural changes that unfold on picosecond and nanosecond time scales. The spatial resolution was sufficient for the faithful imaging of channels with $\sim 10 \text{ nm}$ diameter.

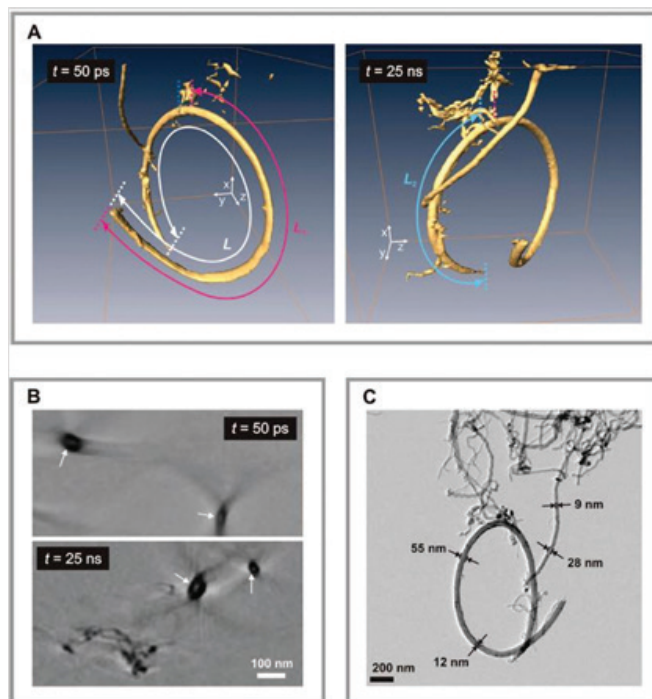


Fig. 13. (A) 3D images of multi-walled carbon nanotubes at different times. The lengths of the respective segments around a fixed area are denoted as L_1 and L_2 . (B) Cross section of the 3D images. Two-dimensional slices in the plane xy are shown. The slice thickness is 4.6 nm . The arrows point to dark areas that show the cross sections of the nanotubes. The spatial resolution is sufficient for the faithful imaging of channels with $\sim 10 \text{ nm}$ diameter. (C) An image taken with a transmission electron microscope [44].

The possibility to create a 3D atomic movie using 4D electron tomography is particularly exciting. It should be emphasized that the pioneering experiments of [44] did not induce irreversible damage in the structure of the nanotube, because the total dose received by the carbon sample during the experiment was about 2 orders of magnitude less than the value at which the irreversible deformations occur. This is a tribute to the extremely high detection efficiency reached in 4D electron microscopy.

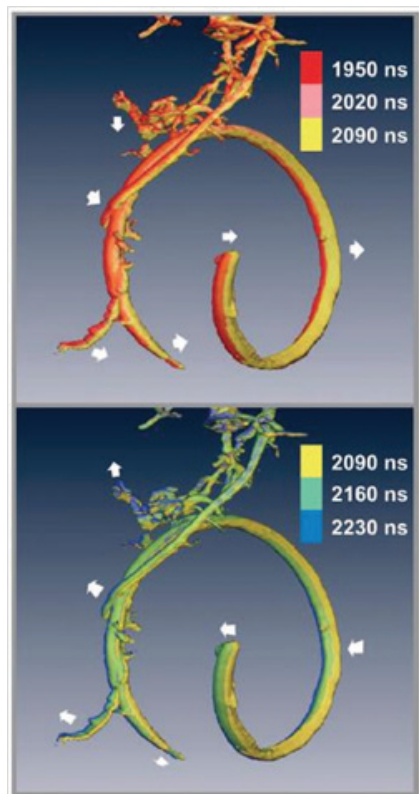


Fig. 14. Mechanical vibrations of a carbon bracelet. The arrows indicate the direction of the individual sections of a carbon nanotube. From [44].

4.5. Plasmonics, nanophotonics and topological phase of matter

The understanding of light–matter interactions near the atomic scale in both space and time is crucial for a variety of different applications, including plasmonics and nanophotonics. It is well known, that rapidly changing electromagnetic fields are the basis of almost any photonic or electronic device operation. These areas hold the promise of advancing both the speed of computers and may also provide techniques to create a new generation of ultrasensitive molecular biosensors. Ultrafast electron microscopy provides a unique window into ultrafast dynamics at the nanoscale: as a result, internal structural, bulk electronic and surface near-field dynamics of these devices can all be obtained with nanometer and femtosecond resolutions. This makes it possible to map the evolution of photonics-related phenomena [45]. The establishment of the time scales of

the different transient structures permits determination of the possible limit of performance, which is crucial for the investigated devices.

The waveform electron microscopy, based on ultrafast electron gun, can be used to visualize electrodynamic phenomena in devices as small and fast as available [46]. The authors observed collective carrier motion and fields with high spatially-temporal resolution using this approach. A collimated beam of femtosecond electron bunches (probe) passes through a metamaterial resonator, excited with a single-cycle electromagnetic pulse (pump). If the probing beam is shorter in duration than half a field cycle, then time-frozen Lorentz forces distort the images quasi-classically. As a result, a pump-probe sequence reveals in a movie the sample's oscillating electromagnetic field vectors with complete information, including their time, phase, amplitude and polarization.

The electronic and structural dynamics in the topological insulator Bi_2Te_3 under strong photoexcitation were characterized with 4D electron microscopy and ultrafast mid-IR laser spectroscopy [47]. The investigated sample characterized as bulk insulators with an electronic conduction surface band have shown a variety of exotic responses in terms of electronic transport when observed under conditions of applied pressure, magnetic field, or circularly polarized light. However, the atomic motions and their correlation between electronic systems in such type of solids under intense laser excitation have not been studied. The artificial and transient modification of the electronic structures in topological insulator via photoinduced atomic motions represents a novel mechanism for providing a comparable level of bandgap control. The results of time-domain crystallography indicate that photoexcitation induces two-step atomic motions: first bismuth and then tellurium center-symmetric displacements. These atomic motions in Bi_2Te_3 trigger 10% bulk band gap narrowing: the obtained data are consistent with ultrafast mid-IR spectroscopy results.

4.6. Imaging of isolated molecules with ultrashort pulsed photoelectron beam

Aligning molecules with intense pulsed laser radiation is a field at the interface between strong laser physics and chemical dynamics with potential applications ranging from high harmonic generation and nanoscale processing to stereodynamics and control of chemical reactions [48]. Intense linearly polarized light induces a dipole force that aligns an anisotropic molecule to the direction of the field polarization [49, 50]. Using femtosecond laser technology, it is possible to spin anisotropic molecules [51, 52]. Rotating the laser polarization causes the molecule to rotate: at high spinning rate, the molecular bond can be broken and the molecules dissociate [51].

Imaging the structure of molecules in transient-excited states remains a challenge due to the extreme requirements for spatio-temporal resolution. Ultrafast electron diffraction from aligned molecules provides atomic resolution and allows for the retrieval of structural information without the need to rely on theoretical models [53–55]. In particular, diffraction from aligned molecules has opened the door to retrieving three-dimensional structures directly from experimental data.

5. Future trend

5.1. Spatial and temporal electron microscopy with additional spectral resolution

The combination of nanoscale spatial resolution with subpicosecond, and eventually femtosecond temporal resolution, forms the basis of the atomic movie. Additional information can be gained when the energy of the electron beam, transmitted through the sample, is measured. Clearly, implementing such a study poses serious experimental challenges.

Therefore, the precedent in this field plays an important role.

This idea was first realized in the work of [56] using a single metal nanostructure. In this experiment, a silver particle of triangular shape with a characteristic length of 130 nm and a thickness of 20 nm was placed on a substrate of graphene (Fig. 15) and irradiated by femtosecond laser pulses with photon energy of 2.4 eV. The optical radiation excites plasma oscillations that were probed by an ultrashort, 10 nm diameter electron beam that was moved across the surface of the sample. The energy gain of the electrons was measured in addition to its spatial and temporal characteristics.

It is important to emphasize that due to the field localized on the surface of a metal particle, the electrons can not only lose kinetic energy, as would be the case with a standard transmission electron microscope, but also acquire energy (Fig. 16). In principle, this process can be controlled by changing the wavelength of the laser radiation. Fundamentally, the accuracy of this procedure is limited by the spectral width of the laser pulse and could reach values approaching 1 meV.

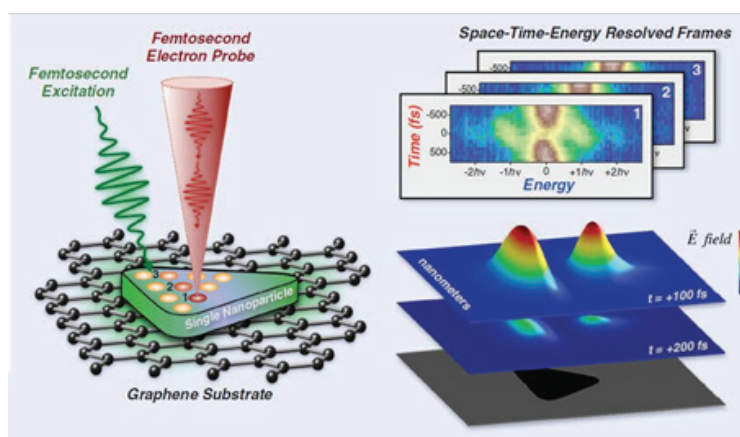


Fig. 15. In the process of ultrafast spectral imaging, a 10 nm electron beam was scanned over the silver particle that was previously excited by a femtosecond laser pulse [56]. For each position of the probe, the change of the kinetic energy of the electrons (i.e. their spectrum) was measured as a function of the delay between the exciting optical and the probe electron pulses. The increase in the energy of the electrons is given in units of the photon energy, being equal to $h\nu = 2.4$ eV. From the article [56].

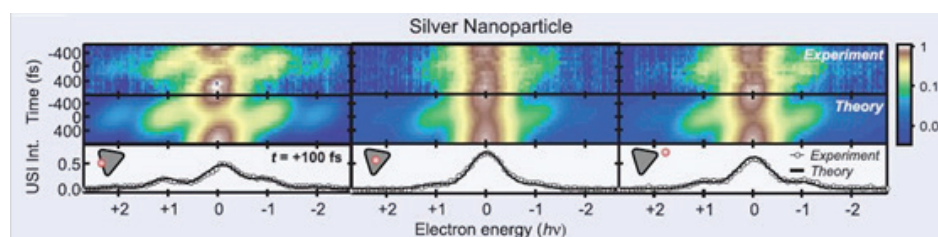


Fig. 16. In [56] spectral and temporal characteristics of silver nanoparticles were investigated. The electron spectra, obtained at a delay of 100 fs after the femtosecond optical pulse, is shown in the bottom traces. Schematically indicated are the positions of the electron beam with respect to the triangular silver particles, which are depicted in gray. From [56].

The measurements by Yurtsever with the co-workers resulted in a map of the plasmonic texture that is generated on the surface of the silver particle, see Fig. 17. As is clearly seen, the field of plasma oscillations is concentrated near the vertices (the cusps) of the triangular particle. The authors report a fairly good agreement with theory. Qualitatively similar results were obtained near the sharp edges of a copper surface irradiated by the laser [56].

The advances of 4D ultrafast electron microscopy in the field of nanoplasmonics and nanophotonics has

enabled observations of the dynamics of photon–matter interactions at the atomic scale with ultrafast resolution in image, diffraction and energy space [57]. In this work the photon–electron interactions have been captured by the method of photon-induced near-field electron microscopy (PINEM) in image and energy space. It should be emphasized, that the PINEM diffraction method paves the way for studies of structural dynamics in reciprocal and energy space with ultrahigh temporal resolution.

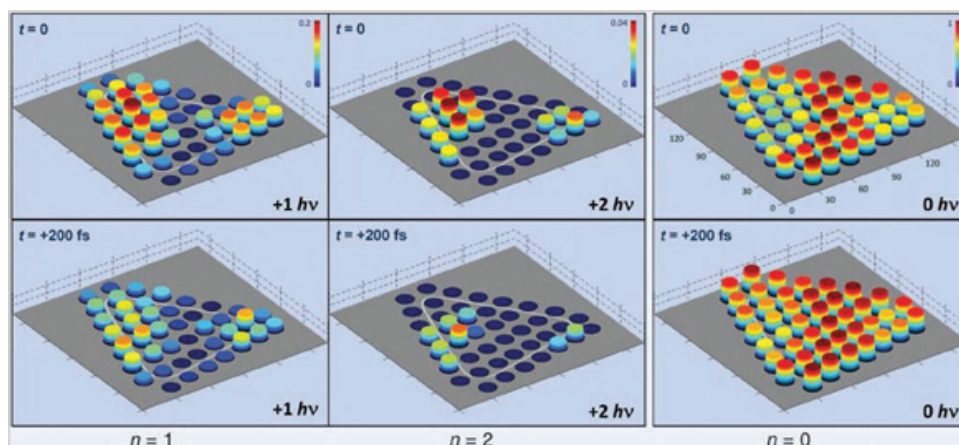


Fig. 17. Factually, plasma oscillations, optically excited in the silver nanostructure by femtosecond laser, were observed using nanolocalized electron bunches. Here, the electron signal is proportional to the height of the corresponding cylinder. For each panel, the energy, acquired as a result of the interaction of the electrons with nanolocalized fields, is shown in the lower right corner. From [56].

5.2. Controlling the motions of free electrons by femtosecond light pulses

Femtosecond lasers play a key role in 4D electron microscopy since they are necessary for the optical initiation of ultrafast processes in the sample as well as to form the ultrashort electron pulses used to probe the progress of the dynamical process. A further use of the pulsed laser radiation is the measurement of the temporal characteristics of the photoelectron bunches. Finally it may be possible to implement additional compression steps that generate shorter electron pulses, potentially reaching into the attosecond regime.

The last statements need to be amplified on, because they imply the possibility of controlling free electrons with a laser beam. At first glance, this statement conflicts with the well-known fact that free electrons cannot absorb the electromagnetic (EM) radiation because the laws of conservation of energy and momentum cannot simultaneously be satisfied. Yet it turns out that free

electrons can scatter EM radiation. From a quantum mechanical point of view, this is the result of stimulated Compton scattering in a strong electromagnetic field.

The possibility to control the translational degrees of freedom of charged particles, in particular of free electrons, by a spatially inhomogeneous electromagnetic field was demonstrated theoretically by Gaponov and Miller in the mid 1950's [58]. The mechanism leads to the ejection of charged particles from the strong field. In the case of high-power laser radiation, the Gaponov-Miller, or ponderomotive (gradient) force (*PF*) [59], which is defined as the spatial gradient of the so-called ponderomotive potential U_p , can reach sufficiently high values to form a basis for the effective control of electron pulses in vacuum.

For non-relativistic electrons, the concept of the ponderomotive potential in a spatially inhomogeneous electromagnetic field, $E = E_0(r)\sin(\omega t)$, can be introduced by averaging the Hamiltonian H over the fast oscillations with frequencies ω and 2ω [24]:

$$H = \langle (p + eE_0(r)\sin(\omega t)/\omega)^2 \rangle / 2m_e = p^2 / 2m_e + [eE_0(r)]^2 / (4m_e\omega^2) = p^2 / 2m_e + U_p \quad (7)$$

Here, m_e and e are the mass and the charge of the electron and $\langle \dots \rangle$ denotes an averaging over optical cycles. As a result, the expression for the PF can be written as:

$$F^{(pond)}(r, t) = -[e^2\lambda^2 / 64\pi^2 m_e \epsilon_0 c^3] \nabla I(r, t) \quad (8)$$

Here ϵ_0 is the dielectric constant, c the speed of light and λ the wavelength of the laser radiation. It follows that for a tightly focused laser pulse with an intensity of

10^{15} W/cm² in the center of a focal spot of 2 μ m diameter (at the level of $1/e$) and $\lambda=800$ nm, the force, $F^{(pond)} \approx 10^{-11}$ N, is approximately equal to the strength of the interaction between two electrons separated by a distance of 5 nm. In this example, the ponderomotive potential is $U_p \approx 60$ eV.

It follows that ultrashort laser pulses allow the control of free electrons in vacuum on a femtosecond time scale. This makes possible both the creation of ultrashort photoelectron bunches and the measurement of their duration [60, 61].

The determination of the temporal characteristics of a pulsed electron beam is based on scanning the time delay between the laser radiation that forms the bunch and the tightly focused laser beam that changes the velocity distribution of the photoelectrons as a result of the *PF*. Such a method compares favorably with a standard streak camera in its technical characteristics and can be used for femtosecond electron beams [61]. In a streak camera, the electrons are deflected by a high-speed and high-voltage electric field with an amplitude of about 2 - 5 kV before reaching a position-sensitive detector. The rate of change of the high electric field determines the temporal resolution of the device. The currently best time resolution is in the subpicosecond range, approaching values of ~ 300 fs [62]. Even so, it is noted that the femtosecond temporal synchronization of the high-voltage electrical pulse in the streak camera and the femtosecond laser pulse that forms the ultrashort photoelectron bunch poses serious technical challenges.

The study of the behavior of the free electrons in spatially inhomogeneous electromagnetic fields began shortly after the development of the theory of Gaponov and Miller. The first experiments were devoted mainly to the possibility of creating traps using microwave technology [63]. Here, special attention was focused on the observation of the passage of the electrons with a certain kinetic energy through the ponderomotive potential, which allowed, for example, one to determine the value of U_p [63, 64]. The first demonstration of scattering of the photoelectrons by the ponderomotive potential, created by an intense sub-nanosecond laser pulse, was done in the study of Bucksbaum et al. [65]. Here the multi-photon ionization of Xe, especially bleeding in the vacuum system, was used to prepare the pulsed photoelectron beam with kinetic energies less than 5 eV. This experiment demonstrated the control of low-energy photoelectrons by an optical ponderomotive potential of about 10 eV.

Special attention should be given to the measurement of the value of the *PF* from the tightly-focused femtosecond laser radiation that interacts with the electrons propagating in vacuum. This may be useful for *in situ* space-time diagnostics of the laser fields of high intensity, and can be used to validate the measurement of ultrashort electron pulse durations based

on the irradiation of the electron bunches with the laser pulses of high intensity. Here it should be noted that the use of laser radiation with intensities of more than 10^{14} W/cm² may be accompanied by the photoionization of the residual gas in the vacuum system and thus by a possible deformation of the electron trajectories that encounter a cloud of charged particles.

The strong electromagnetic field of the focused laser beam can eject electrons from their field-free paths. This is illustrated in Fig. 18, which shows two counter-propagating, tightly-focused laser beams forming a standing wave from which the electron pulse is deflected. The scheme using counter-propagating lasers has two purposes. First, it allows to determine the duration of the initial electron bunch by scanning the timing of the laser pulses that create the standing wave, and using a position-sensitive detector to analyze the rejected, but in general diffused, electron beam components. Secondly, the deflected electron pulses have potentially a shorter time duration than the incident electron pulses.

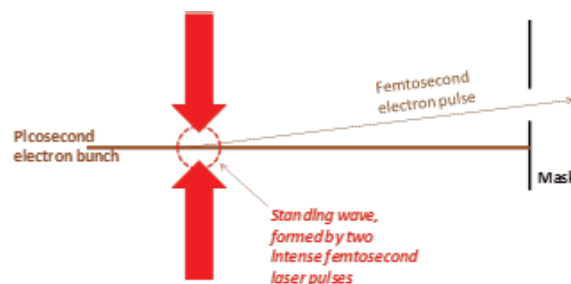


Fig. 18. Deflection of an electron beam as a result of the optical ponderomotive force generated by an ultrashort laser pulse. For illustrative purposes, it is shown the deviation of the electron beam with a very small transverse diameter, when the maximum intensity of the laser field is shifted down somewhat (in the picture). In general, the scattering pattern is more complicated.

Two important remarks should be made here. The scheme in Fig. 18 requires the spatial-temporal matching of two femtosecond laser pulses from two directions and a (sub)picosecond electron bunch from another direction. The use of a single laser beam for the electron scattering would, of course, be simpler. However, in the standing wave the spatial inhomogeneity of the electromagnetic field is about $\lambda/2$, a rather small value that is technically difficult to obtain with a single amplified femtosecond laser beam. For example, a parabolic mirror can usually focus 800 nm amplified femtosecond laser radiation to a spot diameter of $d_{1/e} \sim 6$ microns. Therefore, for a given laser pulse energy, laser wavelength and focusing conditions, the scattering of electrons in a pulsed standing wave will be more pronounced.

A further important consideration relates to the ultimate possibilities of this approach. This is important

because it is rather interesting to know the accuracy of the electron pulse duration measurement as well as the duration of the deflected electron bunch. These characteristics are directly related to the transit time of the fast electrons through the laser focal spot,

$$\tau_{\text{fin}} \approx \tau_{\text{tr}} = d_{1/e} / v_e, \quad (9)$$

where v_e is the speed of the electrons. Using $d_{1/e} = 6 \mu\text{m}$ and $v_e \approx 10^8 \text{ m/s}$ for electrons with 30 keV of kinetic energy, we find $\tau_{\text{tr}} \approx 60 \text{ fs}$. Note that the use of a standing wave formed by two laser beams (Fig. 18) will not lead to a decrease in τ_{fin} , and hence the accuracy of measurement for this example will remain of the order of 100 fs. Therefore, to obtain a femtosecond electron bunches with $\tau \sim 10\text{-}50 \text{ fs}$ it is important to ensure the tight focusing of intense laser radiation, and/or to use electrons with higher kinetic energy.

An alternative way of creating ultrashort electron bunches also employs a standing light wave, but in a collinear geometry [4]. This approach is shown schematically in Fig. 19.

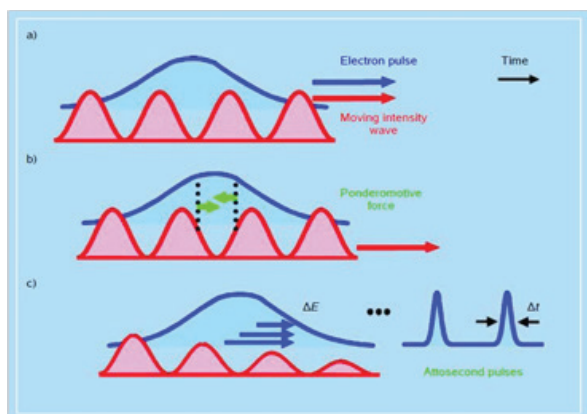


Fig. 19. Schematic diagram of the creation of attosecond electron pulses.

- An electron bunch with sub-picosecond duration is irradiated by two counter-propagating laser beams (forward and after the bunch) with different wavelengths. In the reference frame of the electrons, the wavelengths are the same as a result of the Doppler-effect, and a standing light wave is formed.
- Ponderomotive forces push electrons away from the strong laser field.
- As a result, the compression leads to the formation of electron bunches with attosecond duration. Strictly speaking, the envelope duration of the initial electron bunch remains constant, but importantly, the attosecond spikes appear inside the envelope [66].

(Reprinted figure with permission from [Baum P. and Zewail A.H. Attosecond electron pulses for 4D diffraction and microscopy // Publ. Nat. Acad. Sc. 2007. vol. 104, no. 47, pp. 18409–18414]. Copyright (2007) National Academy of Sciences, U.S.A.)

In this context it should be recalled that on the basis of the uncertainty principle, $\Delta E \Delta t \geq \hbar$, the existence of ultrashort, in this case attosecond, bursts needs a wide spectrum of energy ΔE_e . For example, a bunch with 100 as (10⁻¹⁶ s) duration has at least $\Delta E_e \approx 6 \text{ eV}$. The initial picosecond photoelectron pulse does not exhibit such spectral properties. As shown in Fig. 19, the required broadening is due to the work of the ponderomotive forces [4]. We illustrate this with a simple estimate, by writing down the expression for the work in the traditional sense, where the energy gain of the electrons is equal to $\Delta E_e = F^{(pond)} \tau_p v_e$ (with τ_p the laser pulse duration), and the force is approximately defined as $F^{(pond)} \approx 2U_p / \lambda^*$ (with λ^* the wavelength of the laser radiation in the reference frame of the fast electron). In the conditions of the numerical experiment [4], $U_p \approx 0.2 \text{ eV}$, $\lambda^* = 370 \text{ nm}$, $v_e \approx 10^8 \text{ m/s}$ and $\tau_p = 300 \text{ fs}$, one finds $\Delta E_e \approx 32 \text{ eV}$. The calculated value ΔE_e exceeds by 2 orders of magnitudes the spectral width of "normal" sub-picosecond electron pulse, emitted from the solid photocathode under the action of femtosecond laser radiation.

As considered in the monograph by [4], this scheme is rather elegant. Even so, it is important to emphasize that the measurement of the duration of the formed attosecond electron bursts remains a challenging experimental problem. It is possible that it belongs to the class of experiments in which it is easier to create an ultrashort bunch than to measure it.

Conclusions

Electron microscopy and diffraction with a high temporal resolution have opened the possibility of directly observing processes that occur in non-steady states of materials. A temporal resolution on the order of 100 fs corresponds to the time scale of transitions of a quantum system through an energy barrier of a potential surface, or the formation or breakup of chemical bonds during a chemical reaction. The advances of time-resolved electron microscopy thus open the possibility of investigating the coherent nuclear dynamics of molecular systems and condensed matter [4, 24, 67].

In the past two decades it has become possible to observe the motions of nuclei in time intervals corresponding to the period of oscillation of the nuclei. The changes in the nuclear system during these time intervals probe the fundamental transition from the macroscopic kinetics of a chemical system to the dynamics of the phase trajectory of a single molecule, the molecular quantum state tomography [67–70].

The development of dynamic electron microscopy and the first steps devoted to the progress in the study of structural dynamics of ultrafast processes are illustrated in Fig 20, which summarizes some of the milestones and recent accomplishments.

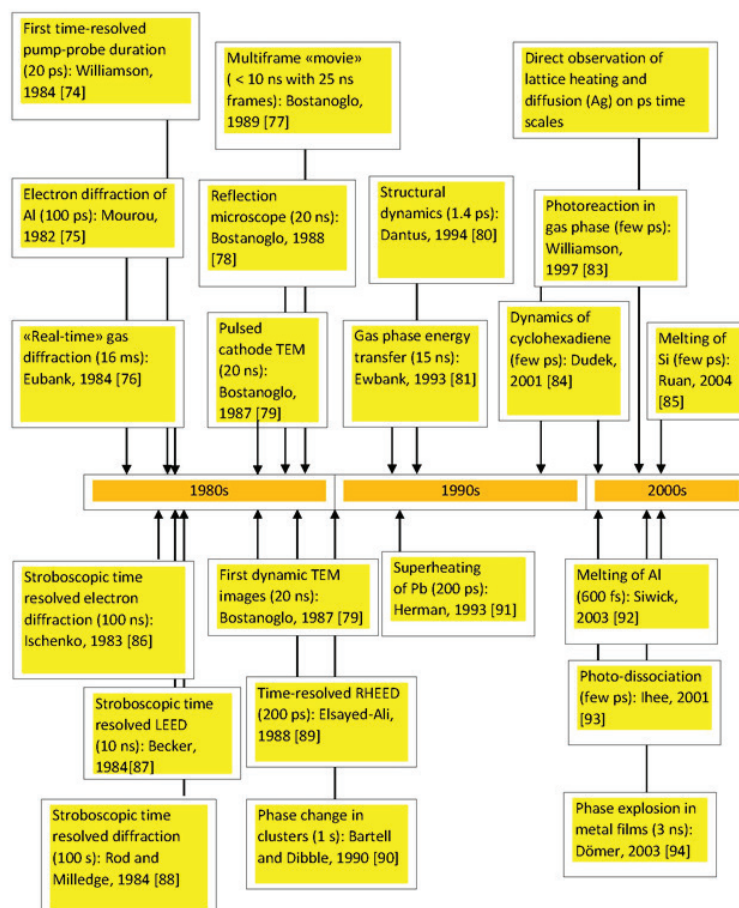


Fig. 20. Chronology of important developments in ultrafast time resolved electron microscopy since 1980's [21].

At present, both the instrument development and the exploration of new phenomena continue at a rapid pace. The methods of ultrafast electron crystallography and electron microscopy with temporal resolution from microseconds to femtoseconds open great opportunities to study the 4D structural dynamics. Very recent advances in the formation of ultrashort electron pulses allow us to reach an attosecond temporal resolution and observe the coherent dynamics of the electrons in molecules [71–73]. It is all but certain that exciting developments in this field will continue into the future.

References:

1. Hawkes P.W., Kasper E. Principles of Electron Optics. V. 1-3. London: Academic Press, 1996. 3710 p.
2. Fultz B., Howe J. Transmission Electron Microscopy and Diffractometry of Materials. Berlin, Heidelberg: Springer Berlin Heidelberg, 2013. 761 p.
3. Parish C.M., Russell P.E. Scanning Cathodoluminescence Microscopy // Advances in Imaging and Electron Physics, V. 147. Elsevier / ed. P.W. Hawkes. Academic Press, 2007. V. 147. P. 1–135.
4. Zewai A.H., Thomas J.M. 4D Electron Microscopy. Imaging in Space and Time. London: Imperial College Press, 2010. 360 p.

There are several research laboratories all over the world experimenting or planning to experiment with ultrafast electron diffraction and possessing electron microscopes adapted to operate with ultrashort electron beams. It should be emphasized that creating a new-generation electron microscope is of crucial importance, because successful realization of this project demonstrates the potential of leading national research centers and their ability to work at the forefront of modern science.

Acknowledgements: Supported by RFBR grant No. 14-22-02035 OFI_m and RFBR grant No. 16 29-1167 OFI_m.

5. Weinstein B.K. Atomic resolution electron microscopy // Sov. Phys. Uspechi Fiz. Nauk. 1987. V. 152. P. 75–122.
6. Brandon J., Kaplan W. Microstructure of Materials. Methods of Research and Monitoring. Moscow : Technosphere, 2004. 384 p.
7. Vlasov A.I., Yelsukov K.A., Kosolapov I.A. Electron microscopy // Library “Nanoengineering” in 17 Books. Book 11. Moscow: Publishing House of Moscow State Technical University named after Bauman, 2011. 168 p.
8. Vlasov A.I., Yelsukov K.A., Panfilov Y.V. Microscopy techniques // Library “Nanoengineering” in 17 Books. Book 1. Moscow: Publishing House of Moscow State Technical University named after

Bauman, 2011. 280 p.

9. Shindo D., Oikawa T. Analytical transmission electron microscopy for materials science. Tokyo, Japan: Springer, 2002. 153 p.

10. Umansky Ya.S., Skakov Yu.A., Ivanov A.N., Rastorgouev L.N. Crystallography, X-ray and electron microscopy. Moscow: Metallurgy, 1982. 632 p. (in Russ.).

11. Heidenreich R.D. Fundamentals of transmission electron microscopy. New York: Interscience Publishers, 1964. 414 p.

12. Hirsch P.B., Howie A., Nicholson R.B., Pashley D.W., Whelan M. J. Electron microscopy of Thin Crystals // *Phys. Today*. 1966. V. 19. № 10. P. 93–94.

13. Locquin M., Langeron M. Handbook of microscopy. London: Butterworths Company Ltd., 1983. 322 p.

14. Spence J.C.H.H. Experimental high-resolution electron microscopy. Oxford University Press, 1988. 427 p.

15. Watt I.M. The principles and practice of electron microscopy. Cambridge: Cambridge University Press, 1997. 484 p.

16. Knoll M., Ruska E. Das Elektronenmikroskop // *Zeitschrift für Phys*. 1932. V. 78. № 5-6. P. 318–339.

17. Thomas G., Goringe M. J. Transmission Electron Microscopy of Materials. New York: Wiley, 1979. 388 p.

18. Amelinks C. Methods of Direct Observation of Dislocations. Wiley, 1968. 440 p.

19. Hawkes P.W. The long road to spherical aberration correction // *Common Sess. Microsc. New Tech. Improv. Microsc. (CST). Biol. Cell*. 2001. V. 93. № 6. P. 432–433.

20. Muybridge E.J. Animal Locomotion, an Electrophotographic investigation of consecutive phases of animal movement. Philadelphia: J.B. Lippincott and Co., 1887.

21. King W.E., Campbell G.H., Frank A., Reed B., Schmerge J.F., Siwick B. J., Stuart B.C., Weber P.M. Ultrafast electron microscopy in materials science, biology, and chemistry // *J. Appl. Phys.* 2005. V. 97. № 11. P. 111101, 1–27.

22. Baskin J.S., Zewail A.H. Seeing in 4D with electrons: Development of ultrafast electron microscopy at Caltech // *Comptes Rendus Phys.* 2014. V. 15. № 2–3. P. 176–189.

23. Grinolds M.S., Lobastov V.A., Weissenrieder J., Zewail, A. H. Four-dimensional ultrafast electron microscopy of phase transitions // *Proc. Natl. Acad. Sci.* 2006. V. 103. № 49. P. 18427–18431.

24. Aseyev S.A., Weber P.M., Ischenko A.A. Ultrafast Electron Microscopy for Chemistry, Biology and Material Science // *J. Anal. Sci. Methods Instrum.* 2013. V. 3. № 1. P. 30–53.

25. Hastings J.B., Rudakov F.M., Dowell D.H., Schmerge J.F., Cardoza J., Castro J.M., Gierman S.M., Loos H., Weber P.M. Ultrafast time-resolved electron

diffraction with megavolt electron beams // *Appl. Phys. Lett.* 2006. V. 89. № 18. P. 184109–184111.

26. Rudakov F.M., Hastings J.B., Dowell D.H., Schmerge J.F., Weber P.M. Megavolt Electron Beams for Ultrafast Time-Resolved Electron Diffraction // *Shock Compression of Condensed Matter / ed. M.D. Furnish, M. Elert, T.P. Russell, C.T. White. AIP*, 2006. V. 845. P. 1287–1292.

27. Weber P.M., Carpenter S.D., Lucza T. Reflectron design for femtosecond electron guns // *Proc. SPIE 2521, Time-Resolved Electron and X-Ray Diffraction*, 23 (September 1, 1995) / ed. Rentzepis P.M. 1995. № 2521.

28. Kassier G.H., Haupt K., Erasmus N., Rohwer E.G., Schwoerer H. Achromatic reflectron compressor design for bright pulses in femtosecond electron diffraction // *J. Appl. Phys.* 2009. V. 105. № 11. P. 113111, 1–10.

29. Gliserin A., Walbran M., Krausz F., Baum P. Sub-phonon-period compression of electron pulses for atomic diffraction // *Nat. Commun.* 2015. V. 6. P. 8723, 1–8.

30. Santala M.K., Reed B.W., Raoux S., Topuria T., LaGrange T., Campbell, G.H. Irreversible reactions studied with nanosecond transmission electron microscopy movies: Laser crystallization of phase change materials // *Appl. Phys. Lett.* 2013. V. 102. № 17. P. 174105–174108.

31. Tokita S., Hashita M., Inoue S., Nishoji T., Otani K., Skabe S. Single-Shot Femtosecond Electron Diffraction with Laser-Accelerated Electrons: Experimental Demonstration of Electron Pulse Compression // *Phys. Rev. Lett.* 2010. V. 105. № 21. P. 215004–215007.

32. Motosuke M., Tetsuya S. Stroboscopic scanning electron microscope: pat. 4538065 USA. Appl. № 470632; 28.02.1983. Date of Patent 27.08.1985

33. Spivak G.V., Shakmanov V.V., Petrov V.I., Lukyanov A.E., Yakunin S. On the application of the gates with the deflection plates in a stroboscopic electron microscopy // *Reports Russ. Acad. Sci. USSR. Phys. Ser.* 1968. V. 32. № 7. P. 1111–1114.

34. Lukyanov A.E., Galstyan V., Spivak G.V. About stroboscopic scanning electron microscopy four-semiconductor structures // *Russ. Technol. Electron.* 1970. № 11. P. 2424–2427.

35. Taheri M.L., Browning N.D., Lewellen J. Symposium on Ultrafast Electron Microscopy and Ultrafast Science. Special Section: Ultrafast Electron Microscopy // *Microsc. Microanal.* 2009. V. 15. № 4. P. 271–271.

36. Knauer W. Boersch effect in electron-optical instruments // *J. Vac. Sci. Technol.* 1979. V. 16. № 6. P. 1676–1679.

37. Lobastov V.A., Srinivasan R., Zewail A.H. Four-dimensional ultrafast electron microscopy // *Proc. Natl. Acad. Sci. U. S. A.* 2005. V. 102. № 20. P. 7069–7073.

38. Zewail A.H. Ultrafast electron diffraction,

crystallography, and microscopy // *Annu. Rev. Phys. Chem.* 2006. V. 57. № 1. P. 65–103.

39. Badali D.S., Gengler R.Y.N., Miller R.J.D. Ultrafast electron diffraction optimized for studying structural dynamics in thin films and monolayers // *Structural Dynamics*. 2016. V. 3. № 3. P. 34302.

40. Hu J., Vanacore G.M., Yang Z., Miao X., Zewail A.H. Transient Structures and Possible Limits of Data Recording in Phase-Change Materials // *ACS Nano*. 2015. V. 9. № 7. P. 6728–6737.

41. Miller R.J.D. Femtosecond Crystallography with Ultrabright Electrons and X-rays: Capturing Chemistry in Action // *Science*. 2014. V. 343. № 6175. P. 1108–1116.

42. Baskin J.S., Park H.S., Zewail A.H. Nanomusical Systems Visualized and Controlled in 4D Electron Microscopy // *Nano Lett.* 2011. V. 11. № 5. P. 2183–2191.

43. *Electron Tomography* / ed. J. Frank. New York: Springer, 2006. 456 p.

44. Kwon O.-H., Zewail A.H. 4D Electron Tomography // *Science* (80-.). 2010. V. 328. № 5986. P. 1668–1673.

45. Barwick B., Zewail A.H. Photonics and Plasmonics in 4D Ultrafast Electron Microscopy // *ACS Photonics*. 2015. V. 2. № 10. P. 1391–1402.

46. Ryabov A., Baum P. Electron microscopy of electromagnetic waveforms. // *Science. American Association for the Advancement of Science*. 2016. V. 353. № 6297. P. 374–377.

47. Hada M., Norimatsu K., Tanaka S., Keskin S., Tsuruta T., Igarashi K. Bandgap modulation in photoexcited topological insulator Bi₂Te₃ via atomic displacements // *J. Chem. Phys.* 2016. V. 145. № 2. P. 24504.

48. Stapelfeldt H., Seideman T. Colloquium: Aligning molecules with strong laser pulses // *Rev. Mod. Phys. American Physical Society*. 2003. V. 75. № 2. P. 543–557.

49. Zon B.A., Katsnel'son B.G. Nonresonant scattering of intense light by a molecule // *JETP*. 1975. V. 42. № 4. P. 595–601.

50. Friedrich B., Herschbach D. Alignment and trapping of molecules in intense laser fields. // *Phys. Rev. Lett. American Physical Society*. 1995. V. 74. № 23. P. 4623–4626.

51. Villeneuve D.M. [et al.] Forced molecular rotation in an optical centrifuge. // *Phys. Rev. Lett. American Physical Society*. 2000. V. 85. № 3. P. 542–545.

52. Korobenko A., Milner A.A., Milner V. Direct Observation, Study, and Control of Molecular Superrotors // *Phys. Rev. Lett.* 2014. V. 112. № 11. P. 113004, 1–5.

53. Hensley C.J., Yang J., Centurion M. Imaging of Isolated Molecules with Ultrafast Electron Pulses // *Phys. Rev. Lett.* 2012. V. 109. № 13. P. 133202.

54. Yang J. [et al.] Imaging of alignment and structural changes of carbon disulfide molecules using

ultrafast electron diffraction // *Nat. Commun.* 2015. V. 6. P. 8172.

55. Centurion M. Ultrafast imaging of isolated molecules with electron diffraction // *J. Phys. B. At. Mol. Opt. Phys.* 2016. V. 49. № 6. P. 62002.

56. Yurtsever A., van der Veen R.M., Zewail A.H. Subparticle ultrafast spectrum imaging in 4D electron microscopy // *Science. American Association for the Advancement of Science*. 2012. V. 335. № 6064. P. 59–64.

57. Liu H., Baskin J.S., Zewail A.H. Infrared PINEM developed by diffraction in 4D UEM. // *Proc. Natl. Acad. Sci. U.S.A.* 2016. V. 113. № 8. P. 2041–2046.

58. Gaponov A.V., Miller M.A. Potential wells for charged particles in a high-frequency electromagnetic field // *Sov. Phys. JETP*. 1958. V. 7. P. 168–169.

59. Kibble T.W.B. Refraction of Electron Beams by Intense Electromagnetic Waves // *Phys. Rev. Lett. American Physical Society*. 1966. V. 16. № 23. P. 1054–1056.

60. Hebeisen C.T., Ernstorfer R., Harb M., Dartigalongue T., Jordan R.E., Miller R.J.D. Femtosecond electron pulse characterization using laser ponderomotive scattering // *Opt. Lett.* 2006. V. 31. № 23. P. 3517–3520.

61. Hebeisen C.T., Sciaini G., Harb M., Ernstorfer R., Dartigalongue T., Kruglik S.G., Miller R.J.D. Grating enhanced ponderomotive scattering for visualization and full characterization of femtosecond electron pulses // *Opt. Express*. 2008. V. 16. № 5. P. 3334–3341.

62. Andreev S.A., Greenfield D.E., Monastyrskiy M.A., Tarasov V.A. Spatial and temporal focusing of femtosecond electron bunches in time-dependent electric fields // *Proceedings of the Seventh International Conference on Charged Particle Optics (CPO-7)*. 2008. V. 1. № 1. P. 273–283.

63. Gekker I.R. Interaction of strong electromagnetic fields with plasmas. Clarendon press, 1982. 324 p.

64. Fedorov M.V. Atomic and Free Electrons in a Strong Light Field. World Scie. Singapore New Jersey London Hong Kong: World Scientific Publishing Co. Pte. Ltd., 1998. 468 p.

65. Bucksbaum P.H., Bashkansky M., McIlrath T.J. Scattering of Electrons by Intense Coherent Light // *Phys. Rev. Lett.* 1987. V. 58. № 4. P. 349–352.

66. Baum P., Zewail A.H. Attosecond electron pulses for 4D diffraction and microscopy // *Proc. Natl. Acad. Sci.* 2007. V. 104. № 47. P. 18409–18414.

67. Ischenko A.A., Bagratashvili V.N., Avilov A.S. Methods for studying the coherent 4D structural dynamics of free molecules and condensed state of matter: article // *Crystallogr. Reports*. 2011. V. 56. № 5. P. 751–773.

68. Ewbank J.D., Schäfer L., Ischenko A.A. Structural and vibrational kinetics of photoexcitation processes using time resolved electron diffraction // *J. Mol. Struct.* 2000. V. 524. № 1. P. 1–49.

69. Ischenko A.A. The study of coherent dynamics of the nuclei by time-resolved electron diffraction. III. Molecular quantum state tomography // *Russ. Trans. Chem. Chem. Technol.* 2009. V. 52. № 9. P. 62–66.
70. Ischenko A.A., Girichev G.V., Tarasov Y.I. Electron diffraction: structure and dynamics of free molecules and condensed matter. Moscow: FIZMATLIT, 2013. 616 p.
71. Ben-Nun M., Cao J., Wilson K.R. Ultrafast X-ray and Electron Diffraction: Theoretical Considerations // *J. Phys. Chem. A.* 1997. V. 101. № 47. P. 8743–8761.
72. Shao H.-C., Starace A.F. Detecting electron motion in atoms and molecules. // *Phys. Rev. Lett. American Physical Society.* 2010. V. 105. № 26. P. 263201–263204.
73. Shao H.-C., Starace A., Madsen L. Ultrafast electron pulse (e,2e) processes // *Bull. Am. Phys. Soc. 43rd Annu. Meet. APS Div. At. Mol. Opt. Phys.* 2012. V. 57. № 5. P. Abstract: N3.00008.
74. Williamson S., Mourou G., Li J.C.M. Time-resolved laser-induced phase transformation in aluminum: *JOUR // Phys. Rev. Lett. American Physical Society.* 1984. V. 52. № 26. P. 2364–2367.
75. Mourou G., Williamson S. Picosecond electron diffraction // *Appl. Phys. Lett.* 1982. V. 41. № 1. P. 44–45.
76. Ewbank J.D., Schäfer L., Paul D.W., Benston O.J., Lennox J.C. Real-time data acquisition for gas electron diffraction // *Rev. Sci. Instrum.* 1984. V. 55. № 10. P. 1598–1603.
77. Bostanjoglo O., Kornitzky J., Tornow R.P. Nanosecond double-frame electron microscopy of fast phase transitions // *J. Phys. E.* 1989. V. 22. № 12. P. 1008–1011.
78. Bostanjoglo O., Heinrich F. A laser pulsed high emission thermal electron gun // *J. Phys. Conf. Ser.* 1988. V. 93. № 1. P. 105–127.
79. Bostanjoglo O., Tornow R.P., Tornow W. Nanosecond-exposure electron microscopy of laser-induced phase transformations // *Ultramicroscopy. North-Holland.* 1987. V. 21. № 4. P. 367–372.
80. Dantus M., Kim S.B., Williamson J.C., Zewail A.H. Ultrafast Electron Diffraction. 5. Experimental Time Resolution and Applications // *J. Phys. Chem. American Chemical Society.* 1994. V. 98. № 11. P. 2782–2796.
81. Ewbank J.D., Luo J.Y., English J.T., Liu R.F., Faust W.L., Schafer L. Time-resolved gas electron diffraction study of the 193-nm photolysis of 1,2-dichloroethenes // *J. Phys. Chem. American Chemical Society.* 1993. V. 97. № 34. P. 8745–8751.
82. Cao J., Hao Z., Park H., Tao C., Kau D., L. Blaszczyk L. Femtosecond electron diffraction for direct measurement of ultrafast atomic motions // *Appl. Phys. Lett.* 2003. V. 83. № 5. P. 1044–1046.
83. Williamson J.C., Cao J., Ihee H., Frey H., Zewail A.H. Clocking transient chemical changes by ultrafast electron diffraction: *JOUR // Nature.* 1997. V. 386. № 6621. P. 159–162.
84. Dudek R.C., Weber P.M. Ultrafast Diffraction Imaging of the Electrocyclic Ring-Opening Reaction of 1,3-Cyclohexadiene // *J. Phys. Chem. A. American Chemical Society.* 2001. V. 105. № 17. P. 4167–4171.
85. Ruan C.-Y., Vigliotti F., Lobastov V.A., Chen S., Zewail A.H. Ultrafast electron crystallography: transient structures of molecules, surfaces, and phase transitions. // *Proc. Natl. Acad. Sci. U.S.A.* 2004. V. 101. № 5. P. 1123–1128.
86. Ischenko A.A., Golubkov V.V., Spiridonov V.P., Zgurskii A.V., Akhmanov A.S., Vabishevich M.G., Bagratashvili V.N. A stroboscopic gas-electron diffraction method for the investigation of short-lived molecular species // *Appl. Phys. B Photophysics Laser Chem.* 1983. V. 32. № 3. P. 161–163.
87. Becker R.S., Higashi G.S., Golovchenko J.A. Low-Energy Electron Diffraction during Pulsed Laser Annealing: A Time-Resolved Surface Structural Study // *Phys. Rev. Lett.* 1984. V. 52. № 4. P. 307–310.
88. Rood A.P., Milledge J. Combined flash-photolysis and gas-phase electron-diffraction studies of small molecules // *J. Chem. Soc. Faraday Trans. 2.* 1984. V. 80. № 9. P. 1145–1153.
89. Elsayed-Ali H.E., Mourou G.A. Picosecond reflection high-energy electron diffraction // *Appl. Phys. Lett.* 1988. V. 52. № 2. P. 103.
90. Bartell L.S., Dibble T.S. Observation of the time evolution of phase changes in clusters // *J. Am. Chem. Soc.* 1990. V. 112. № 2. P. 890–891.
91. Herman J.W., Elsayed-Ali H.E., Murphy E.A. Time-resolved structural study of Pb(100) // *Phys. Rev. Lett.* 1993. V. 71. № 3. P. 400–403.
92. Siwick B.J., Dwyer J.R., Jordan R.E., Miller R.J.D. An atomic-level view of melting using femtosecond electron diffraction // *Science. American Association for the Advancement of Science.* 2003. V. 302. № 5649. P. 1382–1385.
93. Ihee H., Lobastov V.A., Gomez U.M., Goodson B.M., Srinivasan R., Ruan C.-Y., Zewail A.H. Direct imaging of transient molecular structures with ultrafast diffraction. // *Science. American Association for the Advancement of Science.* 2001. V. 291. № 5503. P. 458–462.
94. Dömer H., Bostanjoglo O. High-speed transmission electron microscope // *Rev. Sci. Instrum.* 2003. V. 74. № 10. P. 4369–4372.